# Quantum-Dot-Functionalized Scanning Probes for Fluorescence-Energy-Transfer-Based Microscopy

**Y. Ebenstein, T. Mokari, and U. Banin***

*Institute of Chemistry, the Farkas Center for Light Induced Processes, and the Center for Nanoscience and Nanotechnology, The Hebrew University of Jerusalem, Jerusalem 91904, Israel*

*Received: July 22, 2003; In Final Form: October 8, 2003*

Semiconductor nanocrystals are used to functionalize atomic force microscope (AFM) tips. Such tips may be useful for fluorescence resonance energy transfer (FRET) microscopy. CdSe/ZnS nanocrystals are chemically bound to the surface of an AFM tip by three coating methods utilizing organosilane linker molecules. Binding of nanocrystals by these methods was characterized on silicon and glass surfaces by AFM, scanning electron microscopy (SEM), and optical measurements. The use of mercaptopropyltrimethoxysilane as the linker molecule is found to provide the optimal linking scheme. Via the linking of the nanocrystals to the tip, the unique photophysical properties of the quantum dots and their tunability via chemical synthesis are exploited to create light-emitting scanning probes with controlled emission color, using a single excitation source. The functionalized probes retain their sharpness for high-resolution AFM topography acquisition. These properties are desirable for FRET schemes where the nanocrystals on the tip serve as either FRET donors or acceptors interacting with chromophores on the scanned sample. This interaction provides a contrast mechanism for high-resolution optical imaging in the near field. The potential of these coated tips for FRET-based imaging is demonstrated by localized binding of acceptor dye molecules to the functionalized tips resulting in distinctive FRET signals.

## Introduction

High-resolution optical imaging is an important tool in many fields of physical science, especially biology and medicine.[1] Far-field optical microscopy techniques are used extensively for imaging biological samples with a diffraction-limited resolution of ∼300 nm. Near-field scanning optical microscopy (NSOM)[2,3] allows imaging with resolution below the optical diffraction limit by scanning subwavelength apertures in close proximity to the sample surface. The resolution of NSOM is typically on the order of 100 nm with conventional tapered fiber probes.[4] It is difficult to increase the resolution of this technique to the molecular level because of the finite skin depth of the metal coating surrounding the fiber probe and its low throughput and low damage threshold.[5] This limitation can be overcome by implementing apertureless-NSOM techniques.[6,7] The contrast mechanism of these methods is based on detecting near-field effects that are locally induced by a sharp probe.[8] With the increasingly widespread and robust implementation of atomic force microscopy (AFM) schemes, the apertureless-NSOM techniques also become more accessible.

One approach to enhance optical resolution via apertureless-NSOM is to exploit strongly distance-dependent physical interactions such as FRET (fluorescence resonance energy transfer).[9,10] FRET is widely used in solution experiments[11,12] and in single molecule spectroscopy[13] to determine molecular scale distances in biological samples. The intensity of the FRET signal scales as the inverse sixth power of the distance between donor and acceptor molecules.[14] The range of the FRET process can be estimated from $R_0$, the distance where the interaction is at 50% efficiency, with typical values of 1−10 nm. During the FRET process, energy is transferred nonradiatively through a dipole−dipole interaction from the excited donor chromophore to the acceptor, which fluoresces. Detection of the relative intensities of donor and acceptor fluorescence provides information regarding their relative distance and orientation.[15,16] This sensitivity of FRET to molecular scale distances has been suggested as a contrast mechanism for high-resolution optical imaging.[9,10]

FRET-based microscopy schemes are realized by the immobilization of donor or acceptor chromophores on the tip of a scanning probe microscope used to image the complimentary FRET species on the substrate as seen schematically in Figure 1a. As the functionalized tip approaches a chromophore on the substrate, the FRET interaction leads to donor quenching while inducing acceptor emission, thereby indicating the position of the chromophore with potentially molecular scale resolution.

Several attempts to realize this imaging technique have been reported using pairs of dye molecules. Shubeita et al.[17] coated an NSOM tip with a polymer containing acceptor molecules while Vickery and Dunn[18,19] coated bare fiber probes with a dye containing lipid film or grew a dye containing polymer on silicon nitride AFM tips. In these experiments, a challenging problem is the elimination of the cross-talk between donor and acceptor detection channels caused by direct acceptor excitation and bleeding of the donor fluorescence signal to the acceptor channel. The photostability of the functionalized tips is an additional important issue for the application of the method.

Semiconductor nanocrystals have several advantages over dye molecules as FRET donors. These advantages have also prompted their emerging use as novel biological markers in both in vitro[20,21] and in vivo applications.[22,23] First, the nanocrystals may be tailored, via control of size, composition, and shape,[24−27] to provide exceptional spectral coverage with symmetric emis-

* Author to whom correspondence should be addressed. E-mail: banin@chem.ch.huji.ac.il.

10.1021/jp036135j CCC: $27.50 
Published on Web 12/06/2003

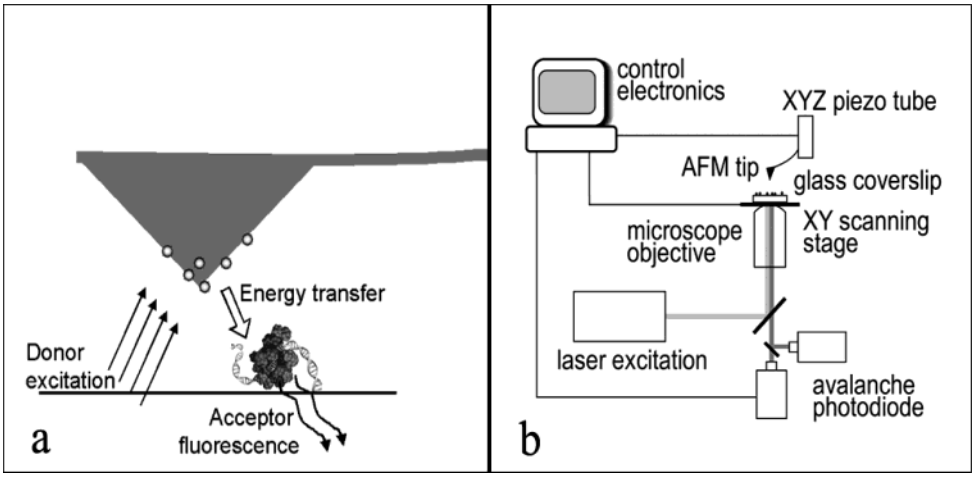


**Figure 1.** (a) Schematic representation of the scheme for FRET-based imaging with tips that are functionalized by semiconductor nanocrystals. (b)Experimental system for correlated AFM and optical measurements.

sion profiles, enabling optimization of donor−acceptor spectral overlap. Additionally, due to their continuous absorption band they may be excited efficiently at shorter wavelength regions where the acceptor dye molecule has minimal absorption cross section thereby reducing direct acceptor excitation and hence donor−acceptor cross-talk. Finally, as already demonstrated in several applications,[23] the nanocrystals are significantly more stable emitters compared to the conventional dye molecules, and as mentioned previously, this is a critical feature for a feasible FRET microscopy scheme. Recently, CdSe/ZnS quantum dots were used as FRET donors in a model protein−protein binding assay demonstrating their advantages for FRET applications.[28]

In this paper, we describe a method to chemically bind CdSe/ZnS nanocrystals to silicon AFM tips for imaging purposes and especially FRET-based microscopy. While writing this paper, it has come to our attention that Shubeita et al. have recently used semiconductor nanocrystals to coat NSOM fiber tips.[29] In their case, the fiber tips were dipped in a polymer solution containing the nanocrystals to yield a 30−100 nm thick layer of nanocrystal-stained polymer. Here, we employ a different approach, using organosilane linker molecules to attach the nanocrystals to conventional AFM tips. The functionalized tips manifest the optical characteristics of the bound nanocrystals while retaining the tip sharpness for high-resolution AFM imaging. We report distinct FRET interactions occurring on the tip apex after collection of acceptor dye molecules from the scanned surface. The high signal-to-noise ratio of this measurement demonstrates the potential of these probes for FRET imaging in the single molecule level.

## Materials and Methods

CdSe/ZnS core/shell nanocrystals and nanorods were prepared by the established methods of colloidal nanocrystal synthesis utilizing high-temperature pyrolysis of organometallic precursors in coordinating solvents.[24,30−32] Glass coverslips were sonicated in detergent solution for 15 min, thoroughly washed in distilled water, and baked in an oven for 5 h at 500 °C yielding highly hydrophilic, optically clean glass. Silicon substrates and silicon AFM tips (MikroMasch NSC11 and CSC12) were activated for 20 s in concentrated nitric acid to yield a clean, hydroxyl rich surface.

The surface of the substrates and the tips were silanized using (aminopropyl)triethoxysilane (APTES, Aldrich) or mercaptopropyltrimethoxysilane (MPTMS, Fluka), either in solution or in the gas phase. Gas-phase silanization of the mercapto- and amine-terminated silanes was performed as follows: Glass coverslips were placed on a Teflon holder inside a glass jar containing a few drops of organosilane. The jar was sealed and heated to 70 °C, and the coverslips were left to react overnight with the silane vapor. Silanization in solution was performed in a 2% (v/v) organosilane/ethanol mixture to which 5% high-purity water was added. The mixture was left to hydrolyze for 5 min after which the glass coverslips were introduced into the solution for an additional 2 min. In the case of MPTMS, rapid polymerization occurred upon addition of water to the mixture as could be seen by the formation of a white polymer-like solid.

After silanization, samples were washed with ethanol (Aldrich), dried with a flow of nitrogen, and incubated for 3−6 h in a $10^{-6}$ M solution of nanocrystals in toluene (Aldrich). After incubation, the samples were washed with toluene to remove unbound particles, dried with nitrogen flow, and stored in the dark under inert conditions until characterized. Dye-stained $\lambda$-DNA ($\lambda$-DNA, New England BioLabs and BOBO-3, Molecular Probes) and dispersed dye molecules (Texas red; BODIPY TR-X, Molecular Probes and ATTO 590, Sigma) were used as test-acceptor chromophores.

For high-resolution scanning electron microscopy (HRSEM) imaging of the tips, the cantilever was broken off of the silicon chip and mounted directly on double-sided carbon tape to minimize charging effects. Measurements were performed on an FEI-Sirion HRSEM with a field emission gun source using voltages of 2−10 kV.

AFM and optical measurements were performed using a system for correlated AFM and scanning fluorescence microscopy (see the illustration in Figure 1b).[33] Briefly, an AFM head (Digital Instruments, Bioscope) is mounted on an inverted microscope (Zeiss, Axiovert 100) equipped with a 100×, 1.4 NA oil immersion objective (Zeiss). The 458 nm line of an argon ion laser (Melles Griot, LAP 321) is focused to a tight spot on the sample surface, which excites the sample in an epi-illumination configuration. Fluorescence is collected by the same objective lens and directed either to a liquid-nitrogen-cooled charge-coupled device (CCD) spectrograph (Princeton Instruments, LN-CCD1100, Acton-SP150) or to a dual-color avalanche photodiode (APD) arrangement (Perkin-Elmer, SPCM-14) for separate detection of donor and acceptor emission. For correlated topography and fluorescence measurements, the AFM tip is positioned within the diffraction-limited excitation spot and the sample is raster scanned by a separate piezo-scanning

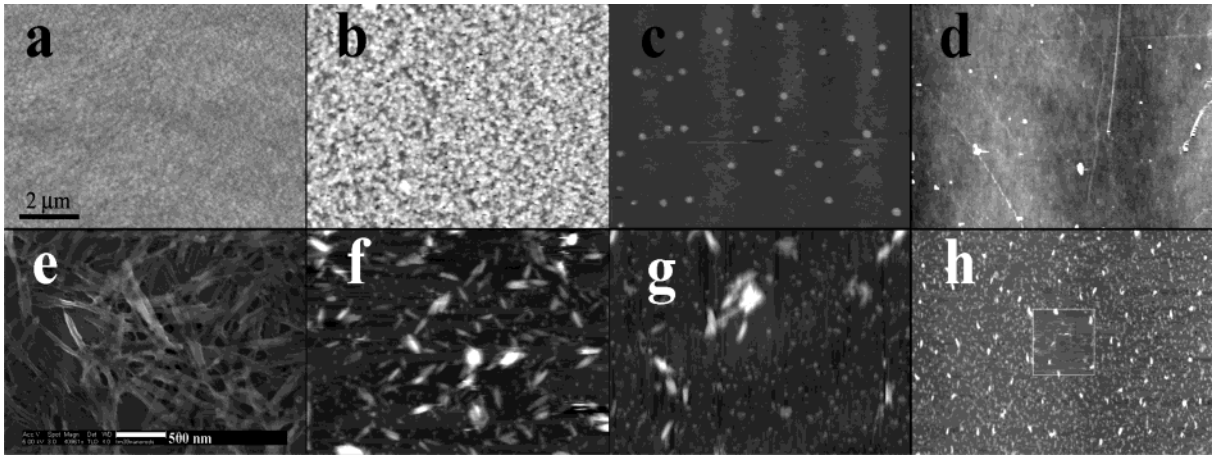


**Figure 2.** AFM images of glass substrates after the various treatments tested: (a) clean glass; (b) glass functionalized with APTES in the gas phase, before incubation in nanocrystal solution; (c) glass functionalized with APTES in solution, before incubation in nanocrystal solution; (d) glass functionalized with MPTMS in the gas phase, before incubation in nanocrystal solution; (e) SEM image of a gas-phase-APTES-functionalized silicon chip; (f) glass functionalized with APTES in the gas phase, after incubation in nanocrystal solution; (g) glass functionalized with APTES in solution, after incubation in nanocrystal solution; (h) glass functionalized with MPTMS in the gas phase, after incubation in nanocrystal solution. In part h, the central region, emphasized with the thin dashed line, shows a 2 $\mu$m $\times$ 2 $\mu$m square that was scanned with stronger constant force resulting in dragging of the particles to the scan borders by the tip. The scale bar in part a applies to all of the AFM images. The height color scale is 10 nm full scale for parts a, c, d, and h, 50 nm full scale for part g, and 100 nm full scale for parts b and f.

stage (Nanonics, Flatscan). This allows for simultaneous recording of both the fluorescence and the topography of the sample and at the same time provides an ideal setup for apertureless-NSOM studies. In the optical data presented here, we primarily report on experiments where the tip was scanned over the diffraction-limited laser spot. This provides the means for the microscopic characterization of the fluorescence from the tip with resolution that is limited by the spot size ($\sim$0.5 $\mu$m), as will be described later.

## Results and Discussion

**Linking of Nanocrystals to AFM Tips.** As a first step toward tip functionalization, an appropriate surface chemistry route to link nanocrystals to $Si/SiO_2$ surfaces was pursued using glass substrates as test-surfaces. Organosilane molecules were reacted with the glass substrates providing a surface similar to that of oxidized silicon cantilevers and then the glass substrates were imaged with AFM to characterize the quality of the molecular coating. Two kinds of terminal groups, amine and thiol, were tested as potential linkers. These end groups, acting as coordinating groups in organic nanocrystal capping ligands, have a known affinity for the nanocrystal surface. The linking is performed by incubating the silanized samples in nanocrystal solution as detailed previously. These samples were further characterized with AFM, SEM, and optical spectroscopy measurements.

Silanized surfaces were characterized with AFM in contact mode. Figure 2 summarizes the AFM characterization of the different coating methods tested on glass coverslips. We used soft cantilevers (0.05 N/m) while applying minimal force. An attempt to use stiffer cantilevers resulted in severe damage to the organic layer, whereas tapping mode AFM measurements resulted in anomalous height data and contrast reversal due to the force effect on the resonance frequency, as we reported in an earlier study.[34] The glass surface before silanization (Figure 2a) is clean and smooth with a mean roughness of 0.45 nm. The gas-phase-APTES-treated coverslip shown in Figure 2b exhibits a rough surface with closely packed polymerized aggregates ranging between 30 and 90 nm in height. SEM imaging of a similarly treated silicon surface revealed rodlike polymerization as seen in Figure 2e. Amine-terminated silanes tend to polymerize, and the polymerization is somewhat reduced using solution-phase linking.

Figure 2c shows the surface after treatment with APTES in solution. Evenly distributed silane aggregates are seen, with heights ranging from 5 to 10 nm and an average density of $\sim$2 aggregates per $\mu m^2$. A considerably improved surface was obtained for the gas-phase-MPTMS-treated glass. The roughness of the mercaptosilane-functionalized surface is on the order of 0.3 nm and shows only occasional aggregation.

Substrates treated similarly to those discussed previously were characterized with AFM after incubation in similar nanocrystal solutions (in this case we used a $10^{-6}$ M solution of 4 nm CdSe/ZnS dots). The bare glass surface showed only occasional large aggregates that were not washed away. Isolated small particles were not detected. It is important to note that it is very difficult to image unbound nanocrystals with contact mode AFM because of dragging of the particles by the tip.[35] AFM parameters had to be carefully tuned to avoid dragging the particles on the substrate. In contrast to the bare glass, the silanized substrates show extensive binding of nanocrystals on all of the surfaces. In these cases, dragging was much less pronounced and we did not need to exercise special care in the AFM imaging to avoid it, indicating that the nanocrystals are bound to the substrates with a relatively strong interaction. As may be expected from the images of the silanized substrates, the MPTMS-treated glass (Figure 2h) exhibits the most uniform coverage of nanocrystals with no aggregation, whereas the gas-phase-APTES-treated glass (Figure 2f) exhibits large nanocrystal aggregates. In Figure 2h, a stronger lateral force was applied by the tip in the central 2 $\mu$m region resulting in detachment of bound particles that were dragged by the tip to the borders of the scanned area. Fluorescence measurements of the samples, excited at 514 nm, showed photoluminescence (PL) that is similar on all substrates and closely matches the PL of the same nanocrystals in solution.

From the results of these silanization experiments, it is evident that the gas-phase deposition of MPTMS is the most appropriate method for tip coating. This method is easy to implement and yields high-quality surface morphology. Minimum exposure to air and water should be exercised after silanization to avoid

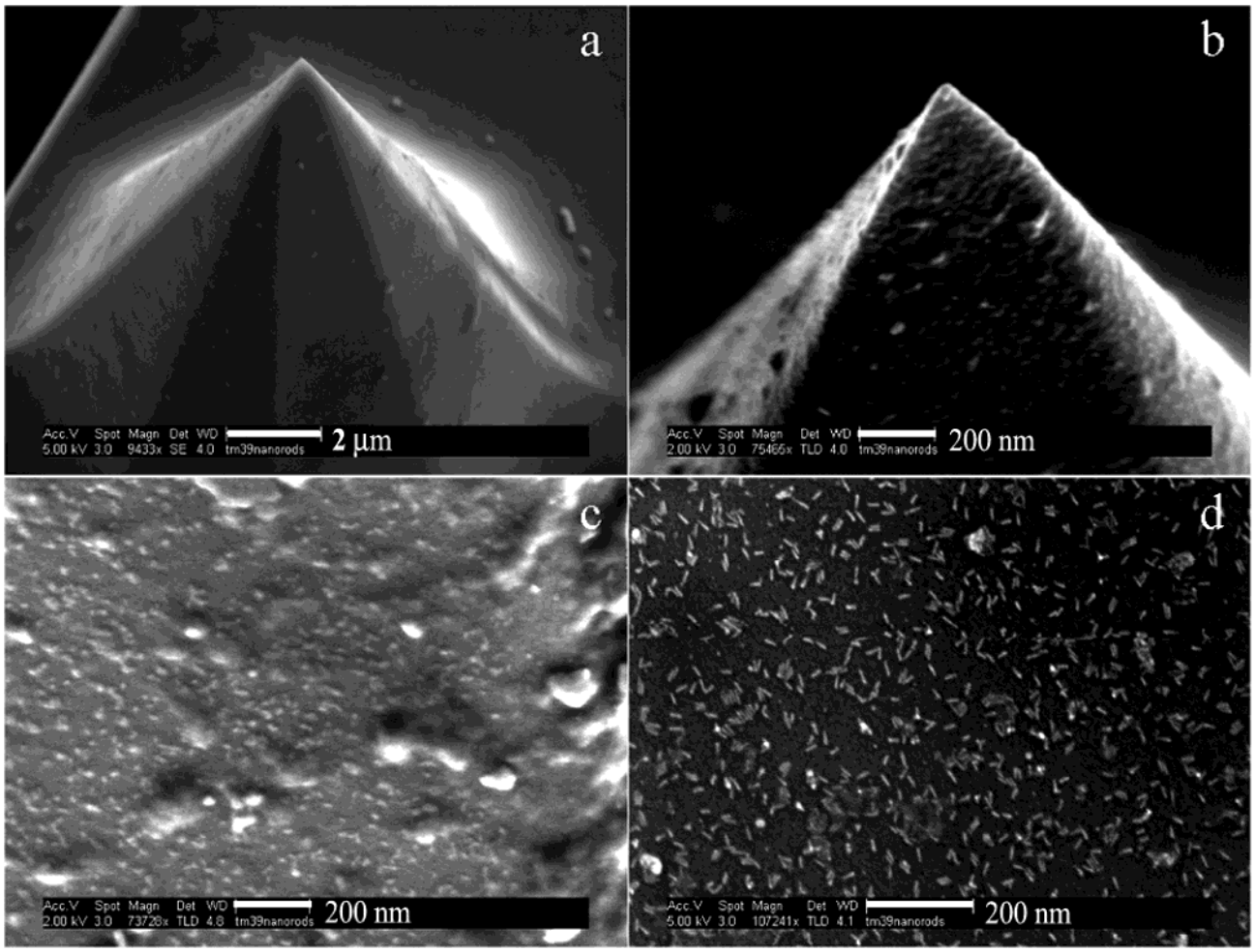


**Figure 3.** HRSEM images of an MPTMS-nanorod-functionalized tip: (a) general view; (b−d) close up of the tip apex, tip surface, and cantilever, respectively. Because of charging effects, nanorods are resolved more clearly as the imaging is performed closer to the conducting substrate.

end group oxidation and contamination. The high affinity of the mercapto end group to the nanocrystal surface results in high nanocrystal coverage after 3 h of incubation in the nanocrystal solution. No effects on nanocrystal emission were observed. Using this coating method, AFM tips emitting various colors are easily prepared and may be tailored for specific applications.

Direct characterization of the functionalized tips was performed by HRSEM imaging. Figure 3 shows HRSEM images of a functionalized AFM tip treated with MPTMS and coated with nanocrystals. For imaging purposes, this tip was functionalized with nanorods 4 nm in diameter and 22 nm long. It is clear from parts a and b of Figure 3 that the tip retains its general features and sharpness. Nanorods are identified on the tip apex, but because of charging effects, it is difficult to resolve them. They can be clearly resolved on the tip surface and most clearly on the tip cantilever which has the best contact to the conducting tape and therefore minimal charging problems (parts c and d of Figures 3, respectively). Functionalization of the tip surface is therefore successfully implemented and nicely controlled where aggregation can be avoided. We note that the density of the nanocrystals coating the tip can be controlled by modifying the incubation time and concentration of the nanocrystal solution.

The emission spectrum from the same tip discussed previously was measured with the fluorescence microscope setup and is traced in a dashed line in Figure 4. The fluorescence is similar to that observed in solution for the same sample. To demonstrate the general applicability of this approach for functionalizing AFM tips with nanocrystals and nanorods, we performed similar linking experiments for other nanocrystals. Fluorescence from three more coated tips is also presented in Figure 4. The emission color from the tip is easily controlled by depositing nanocrystals of different sizes, and in this case, the emission spans the range from 556 nm for 3.5 nm CdSe/ZnS dots to 609 nm for 4 nm × 22 nm rods. The emission range of the functionalized tips could easily be extended to cover a broad range of wavelengths by connecting nanocrystals of other semiconductors from the wide variety of such samples that is presently available. Because the surface chemistry of II−VI, III−V, and IV−VI semiconductor nanocrystals is similar, the same functionalization scheme could be used to provide tips with emission from the blue to the near-infrared (NIR). Metal nanocrystals, for example, gold or silver, could be linked in similar fashion for microscopy schemes such as surface-enhanced Raman microscopy.[36]

An additional important issue for the functionalization process is that it should not hamper the performance of the AFM tip in topographic imaging. This was tested by imaging stretched DNA on glass with the tip emitting at 556 nm as shown in the top left inset of Figure 4. A cross section of the DNA image reveals a width at half-maximum of 26 nm, similar to that achieved with an untreated tip and indicating that the tip remains sharp and capable of high-resolution AFM imaging.

**FRET Processes Observed on the Tip.** We next turn to observe FRET processes with the functionalized tips. While scanning a substrate with dye molecules under the tip, we found

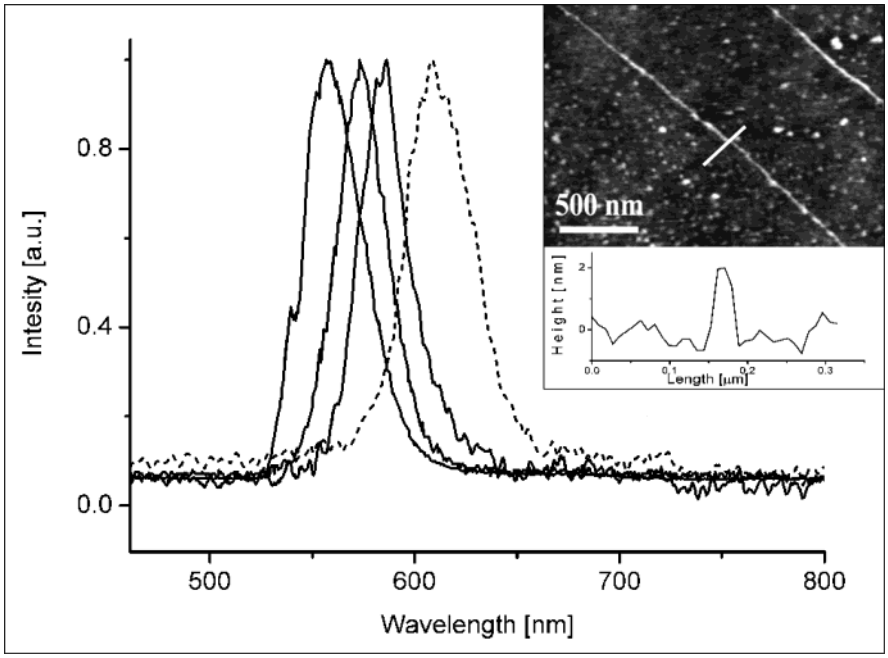


**Figure 4.** Emission spectra of four functionalized tips ranging from 556 to 609 nm. From left to right, tips were functionalized with CdSe/ZnS nanocrystals of 3.5, 4, and 4.5 nm in diameter. The spectrumrepresented by the dashed line corresponds to that of the 22 nm × 4 nm rods on the tip imaged in Figure 3. The inset shows an AFM image and line section of stretched DNA on glass acquired by the tip emitting at 556 nm. Sharpness of the tip for AFM topography is maintained.

that the tip collects dye molecules. For FRET microscopy, a means for avoiding such collection is required, and we are presently studying methods to strongly bind the acceptor molecules to reduce this undesired process. Therefore, the experiments reported here employ an experimental scheme that involves collecting acceptor dye molecules on the tip apex and then imaging a projection of the tip by scanning it over a diffraction-limited excitation spot and collecting its emission. The FRET process in this case is seen to occur on the tip itself at positions where the dye molecules were collected on the nanocrystal-functionalized tip.

For these FRET measurements, the collected emission was split to two APD detectors using a 610 nm dichroic mirror. With this setup, donor (nanocrystal) and acceptor (dye) fluorescence is detected nearly independently.[37] A dilute ethanol solution of ATTO 590 (Sigma) dye was spin cast on a clean glass coverslip resulting in separated single acceptor dye molecules. A tip functionalized with 4.5 nm diameter CdSe/ZnS nanocrystals emitting at 570 nm was scanned over the glass surface, raster scanning an area containing approximately 10 dye molecules. In the scanning process, a few dye molecules stick to the tip apex in close proximity to one or more of the nanocrystal donors attached to the tip, thus creating a FRET pair. At this stage, the tip is scanned over the excitation spot while its fluorescence is collected pixel by pixel in the two APDs to create simultaneously the images shown in parts a and b of Figure 5. We emphasize that such a scan does not provide a microscopic image of the substrate, but rather of the tip itself. The inherent resolution is limited by the size of the laser spot in this case and does not fully manifest the potential high resolution of FRET microscopy. The image in Figure 5b, showing data collected in the (blue) donor channel, represents mainly nanocrystal emission. It can be seen that the emitting area is approximately "n-shaped" with a size of about 1.5 $\mu$m × 1 $\mu$m and consists of a bright right lobe and a weaker left region. This reflects the contour of the tip apex. The relative intensities are shown in the line section above the image. Figure 5a, showing data collected in the (red) acceptor channel, represents acceptor dye emission together with the red nanocrystal emission tail. Here, the strongest signal shows up on the left side and correlates spatially to the weaker part in the donor image. This can be clearly seen if the two images are superimposed as shown in Figure 5c. Here, the green color represents donor emission while red represents acceptor emission, indicating that during scanning acceptor dye molecules have been collected at a specific region of the tip. Remember that the resolution of this experiment is limited by the laser spot diameter. Therefore, even acceptor signals generated by a single dye molecule will appear as a 400 nm diameter emission spot in the collected image.

These scans of the tip show FRET between the nanocrystals and the dye molecules on the tip itself, leading to enhanced dye emission along with quenching of the nanocrystal emission. This observation was verified spectrally by taking localized spectra from different regions of the tip and from isolated dye molecules on the surface. Figure 5d demonstrates this FRET interaction; the green dashed line shows a spectrum, taken from the right tip region, that is clearly dominated by the donor nanocrystal emission peak centered at 574 nm. The solid red line shows a spectrum that was taken from the region with maximum emission in the acceptor channel, and both donor and acceptor contributions are seen. The dotted black line is a spectrum of a single dye molecule with a peak at 610 nm that was recorded with higher excitation power due to the low direct excitation by the 458 nm laser line.

The distribution of dye molecules on the substrate is 0−1 molecules per $\mu$m$^2$; therefore, only a few dye molecules could have been collected by the tip on the scanned area. Furthermore, judging from the density of attached nanocrystals studied previously, only a few particles attached to the apex area can contribute to the FRET interaction. This, together with the observed simultaneous enhancement and quenching of the acceptor and donor emission respectively, indicates that localized FRET interaction is observed to take place on the tip. Disengaging the tip from the surface results in disappearance of the FRET signal, verifying that this interaction is indeed occurring on the tip surface. The inset in Figure 5d shows another case where a

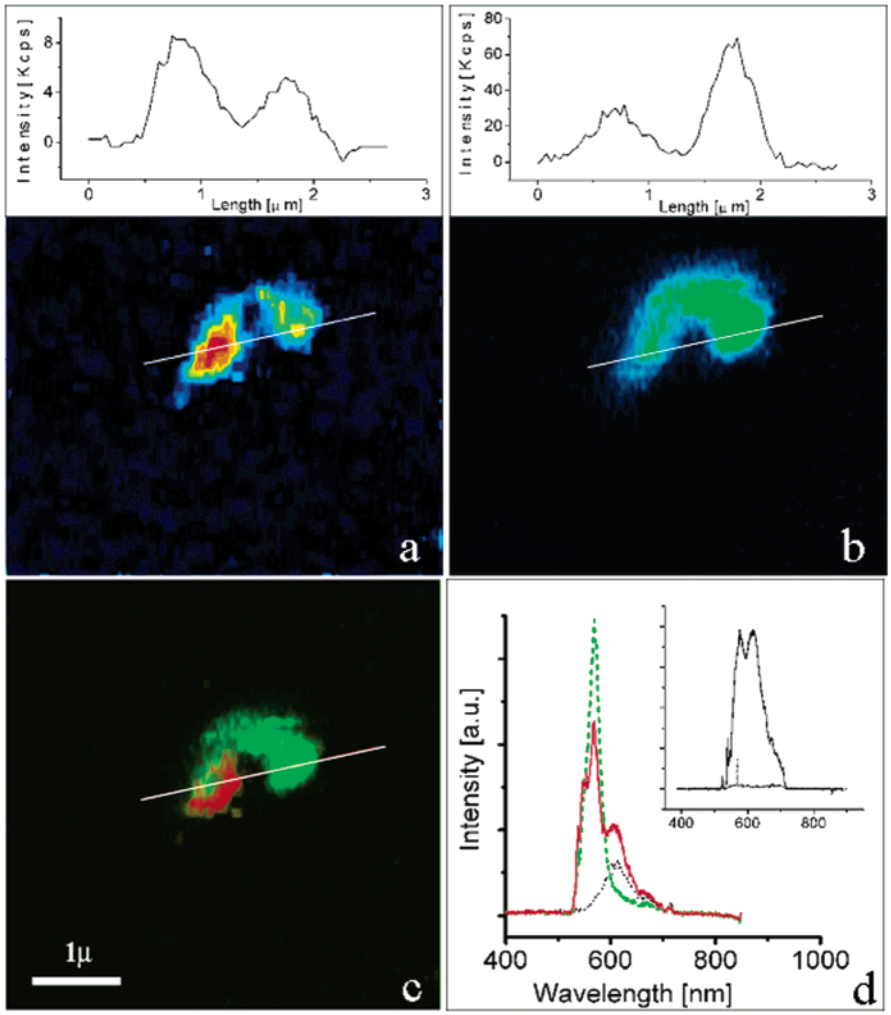


**Figure 5.** Demonstration of local FRET between nanocrystals on the functionalized tip and dye molecules collected by them while scanning the tip over the diffraction-limited laser illumination spot: (a) fluorescence image of the tip acquired in the acceptor channel and its line section showing dominant acceptor signal intensity in the left region; (b) fluorescence image of the tip acquired in the donor channel and its line section showing dominant donor signal intensity in the right region; (c) superimposed image of the tip representing spatially localized donor (green) and acceptor (red) emission from the tip; (d) spectra taken from a single dye molecule on the surface emitting at 610 nm (black, dotted line), the central tip region showing pure nanocrystal emission at 574 nm (green, dashed line), and the left tip region where both peaks are resolved, demonstrating the FRET interaction (red, solid line). The inset in part d shows another case where the FRET signal is detected (solid line) and disappears when the tip is retracted from the surface (dashed line), indicating that the fluorescence signal is coming from the tip and further showing that dye molecules are collected by the tip.

functionalized tip collected dye molecules from the sample surface during scanning. The solid and dashed lines are spectra of the tip while engaged and disengaged from the surface, respectively.

We have not succeeded so far in fully implementing the potential of the FRET microscopy scheme with the nanocrystal-functionalized tips because of the problemof the dye molecules sticking to the tip while scanning. However, the experiments performed so far demonstrate that the strong distance dependence of FRET interaction together with tip geometry serves to confine the active photonic volume for FRET to the tip apex. Clearly, the functionalized tips emit light with a $\mu$m scale area reflecting their contour within the excitation spot; yet, the FRET signal observed is localized in an area equivalent to the excitation spot size with a diameter of approximately 400 nm. The fact that in this experiment all FRET signals come from the tip, which is scanned over the excitation spot, limits our resolution to the diffraction-limited spot size. It may very well be, as seen from SEM images of the tips, that for surface immobilized acceptors resolution could be significantly improved by over 1 order of magnitude. The main drawback of this technique for imaging single molecules so far is their tendency to be collected by the nanocrystals on the functionalized tip. This was verified in solution experiments where we observed FRET signals from a mixed solution of Texas red dye molecules and nanocrystals, indicating spontaneous, nonspecific binding of dye to the nanocrystal surface.[38] Experiments are currently in progress where we are attempting to develop schemes that allow optical imaging of immobilized acceptor molecules.

Selective attachment of single nanocrystals to the tip apex is also under investigation in our lab. Such tips can act as nanometric light sources for NSOM as demonstrated by Sandoghdar et al. for a single dye molecule.[39] For FRET-based imaging, a large coated area can still result in a small active volume localized at the tip apex as shown in Figure 5, based on the short range of the FRET interaction.

## Conclusions

We developed a simple method for the functionalization of AFM tips with semiconductor nanocrystals. The resulting tips

remain sharp, retaining the benefits of AFM imaging while possessing photophysical properties of the attached nanocrystals. Emitting probes with various emission colors can be prepared and easily tailored for specific applications. These functionalized probes are especially attractive for imaging schemes based on FRET. The potential use of semiconductor nanocrystals as donors in such an imaging scheme was demonstrated through the observation of FRET taking place to dye molecules collected by the tip. These measurements show high signal-to-noise ratio for FRET detection, enabling high collection efficiency and sensitivity to single-molecule signal levels. The nature of the FRET interaction serves to confine the active photonic volume to the tip apex, thus enhancing potential imaging resolution with such probes.

**Acknowledgment.** We thank Mila Palchan of the Unit for Nanoscopic Characterization for performing the HRSEM imaging. We thank a reviewer for useful suggestions to clarify the results. This research was supported by the Israel Science Foundation (Grant No. 99/00-12.5).

**Supporting Information Available:** Experimental details and results from solution FRET experiments demonstrating nonspecific, spontaneous binding of Texas red dye molecules to CdSe/ZnS nanocrystals. This material is available free of charge via the Internet at http://pubs.acs.org.

## References and Notes

(1) Herman, B. *Fluorescence Microscopy*, 2nd ed.; Bios Scientific Publishers: Oxford, U.K., 1998.
(2) Lewis, A.; Isaacson, M.; Harootunian, A.; Murray, A. *Ultramicroscopy* **1984**, *13*, 227.
(3) Betzig, E.; Trautman, J. K.; Harris, T. D.; Weiner, J. S.; Kostelak, R. L. *Science* **1991**, *251*, 1468.
(4) Dunn, R. C. *Chem. Rev.* **1999**, *99*, 2891.
(5) Novotny, L.; Pohl, D.; Hecht, B. *Opt. Lett.* **1995**, *20*, 970.
(6) Zenhausern, F.; O'Boyle, M. P.; Wickramasinghe, H. K. *Appl. Phys. Lett.* **1994**, *65*, 1623.
(7) Furukawa, H.; Kawata, S. *Opt. Commun.* **1998**, *148*, 221.
(8) Sanchez, E. J.; Novotny, L.; Xie, X. S. *Phys. Rev. Lett.* **1999**, *82*, 4014.
(9) Kopelman, R.; Lewis, A.; Lieberman, K. *J. Lumin.* **1990**, *45*, 298.
(10) Sekatskii, S. K.; Letokhov, V. S. *JETP Lett.* **1996**, *63*, 319.
(11) Stryer, L.; Haugland, R. P. *Proc. Natl. Acad. Sci. U.S.A.* **1967**, *58*, 719.
(12) Selvin, P. R. *Methods Enzymol.* **1995**, *246*, 300.
(13) Ha, T.; Enderle, T.; Ogletree, D. F.; Chemla, D. S.; Selvin, P. R.; Weiss, S.; *Proc. Natl. Acad. Sci. U.S.A.* **1996**, *93*, 6264.
(14) Forster, T. *Modern Quantum Chemistry*; Academic: New York, 1965.
(15) Weiss, S. *Science* **1999**, *283*, 1676.
(16) Deniz, A. A.; Laurence, T. A.; Beligere, G. S.; Dahan, M.; Martin, A. B.; Chemla, D. S.; Daswon, P. E.; Schultz, P. G.; Weiss, S. *Proc. Natl. Acad. Sci. U.S.A.* **2000**, *97*, 5179.
(17) Shubeita, G. T.; Sekatskii, S. K.; Dietler, G.; Letokhov, V. S. *Appl. Phys. Lett.* **2002**, *80*, 2625.
(18) Vickery, S.A.; Dunn, R. S. *Biophys. J.* **1999**, *76*, 1812.
(19) Vickery, S. A.; Dunn, R. S. *J. Microsc.* **2001**, *202*, 408.
(20) Chan, W. C. W.; Nie, S. *Science* **1998**, *281*, 2016.
(21) Bruchez, M.; Moronne, M.; Gin, P.; Weiss, S.; Alivisatos, A. P. *Science* **1998**, *281*, 2013.
(22) Larson, D. R.; Zipfel, W. R.; Williams, R. M.; Clark, S. W.; Bruchez, M. P.; Wise, F. W.; Webb, W. W. *Science* **2003**, *300*, 1434.
(23) Dubertret, B.; Skourides, P.; Norris, D. J.; Noireaux, V.; Brivanlou, A. H.; Libchaber, A. *Science* **2002**, *298*, 1759.
(24) Murray, C. B.; Norris, D. J.; Bawendi, M. G. *J. Am. Chem. Soc.* **1993**, *115*, 8706.
(25) Cao, Y. W.; Banin, U. *J. Am. Chem. Soc.* **2000**, *122*, 9692.
(26) Peng, X. G.; Manna, L.; Yang, W. D.; Wickham, J.; Scher, E.; Kadavanich, A.; Alivisatos, A. P. *Nature* **2000**, *404*, 59.
(27) Kan, S. H.; Mokari, T.; Rothenberg, E.; Banin, U. *Nature Mater.* **2003**, *2*, 155.
(28) Willard, D. M.; Carillo, L. L.; Jung, J.; Van Orden, A. *Nano Lett.* **2001**, *1*, 469.
(29) Shubeita, G. T.; Sekatskii, S. K.; Dietler, G.; Potapova, I.; Mews, A.; Basché, T. *J. Microsc.* **2003**, *210*, 274.
(30) Hines, M. A.; Guyot-Sionnest, P. *J. Phys. Chem.* **1996**, *100*, 468.
(31) Talapin, D. V.; Rogach, A. L.; Kornowski, A.; Haase, M.; Weller, H. *Nano Lett.* **2001**, *1*, 207.
(32) Mokari, T.; Banin, U. *Chem. Mater.* **2003**, *15*, 3955.
(33) Ebenstein, Y.; Mokari, T.; Banin, U. *Appl. Phys. Lett.* **2002**, *80*, 4033.
(34) Ebenstein, Y.; Nahum, E.; Banin, U. *Nano Lett.* **2002**, *2*, 945.
(35) Junno, T.; Anand, S.; Deppert, K.; Montelius, L.; Samuelson, L. *Appl. Phys. Lett.* **1995**, *66*, 3295.
(36) Anderson, M. S. *Appl. Phys. Lett.* **2000**, *76*, 3130.
(37) Enderle, T.; Chemla, D. S.; Ha, T.; Magowan C.; Weiss, S. *Proc. Natl. Acad. Sci. U.S.A.*, **1997**, *94*, 520.
(38) See the Supporting Information for details.
(39) Michaelis, J.; Hettich, C.; Mlynek, J.; Sandoghdar V. *Nature* **2000**, *405*, 325.